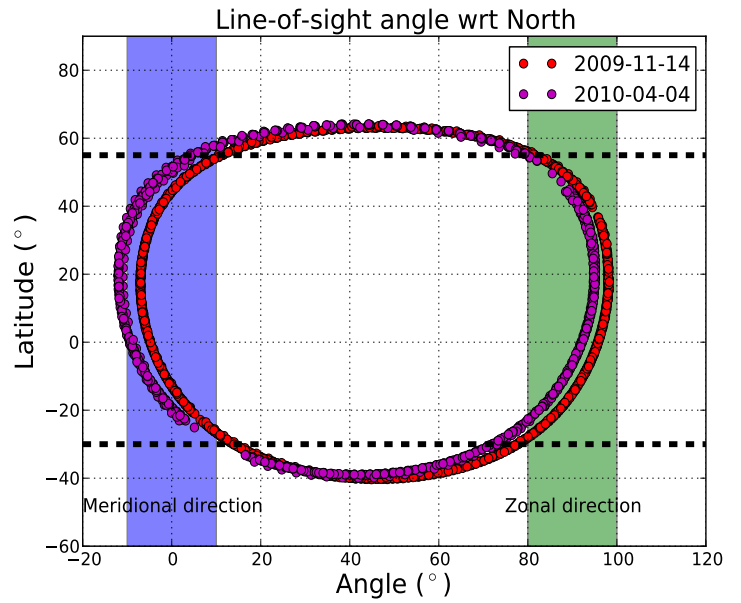
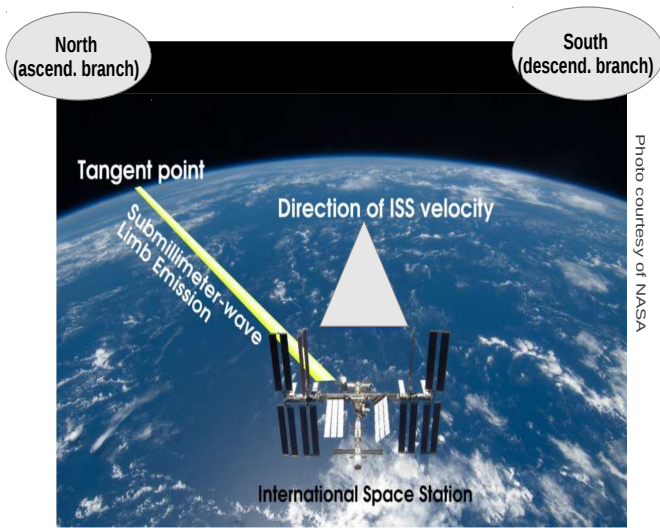
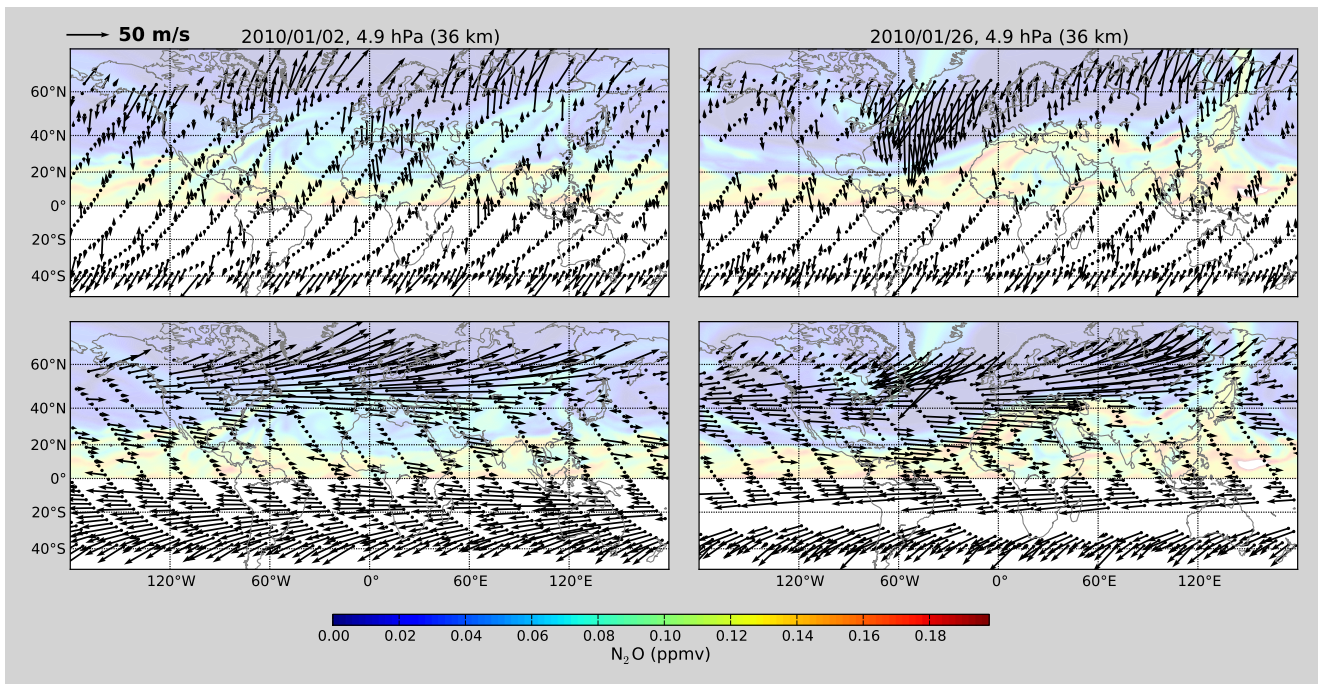


**Fig. 1.** The height coverage and estimated precision of past, current and future wind measuring instruments (reported validated precisions are indicated where possible, darker values are theoretical values). HRDI (Ortland et al., 1996) and WINDII (Shepherd et al., 1993) were on the UARS satellite and operated from September 1991–June 2005, TIDI (Niciejewski et al., 2006) operates on the TIMED satellite from 2002–present, AURA-MLS (Wu et al., 2008) operates on the AURA satellite from July 2004–present (note that wind is not a standard product), SMILES operated on the ISS from September 2009–April 2010, Aeolus is ESA mission (Stoffelen et al., 2005) planned for 2013 and SWIFT (McDade et al., 2001) is under study in Canada.



**Fig. 2.** Left panel: Representation of the limb observation geometry (adapted from <http://smiles.nict.go.jp/pub/about/principles.html>). The ISS orbit inclination is  $51.6^\circ$  with respect to the equator and the SMILES line-of-sight is tilted by  $45^\circ$  on the left side of the forward direction. The tangent point is at a distance of  $\sim 2000$  km from the ISS. North (South) direction is indicated for the ascending (descending) orbit branch. Right panel: latitudinal variation of the line-of-sight angle with respect to the North direction on 14 November 2009 (red circles) and on 4 April 2010 (magenta circles). The blue (green) region indicates the region where the line-of-sight is at  $\pm 10^\circ$  about the meridional (zonal) direction. The thick dashed horizontal lines indicate the latitude range between  $30^\circ\text{S}$  and  $55^\circ\text{N}$ .



**Fig. 3.** Typical line-of-sight wind vectors retrieved at 5 hPa (~36 km) on 2 January 2010 (left column) and on 26 January 2010 (right column). The orientation of the arrows is that of the wind component along the line-of-sight. The length of the arrows is proportional to the amplitude of the corresponding line-of-sight wind (the same proportional factor is applied at all latitudes). The upper (lower) panels correspond to the ascending (descending) branch of the orbit where the line-of-sight is near the meridional (zonal) direction between ~35°S to ~55°N. The background colour shows the Northern N<sub>2</sub>O distribution from the assimilated Odin/SMR measurements in a model driven by ECMWF winds at the isentropic surface of 850 K.

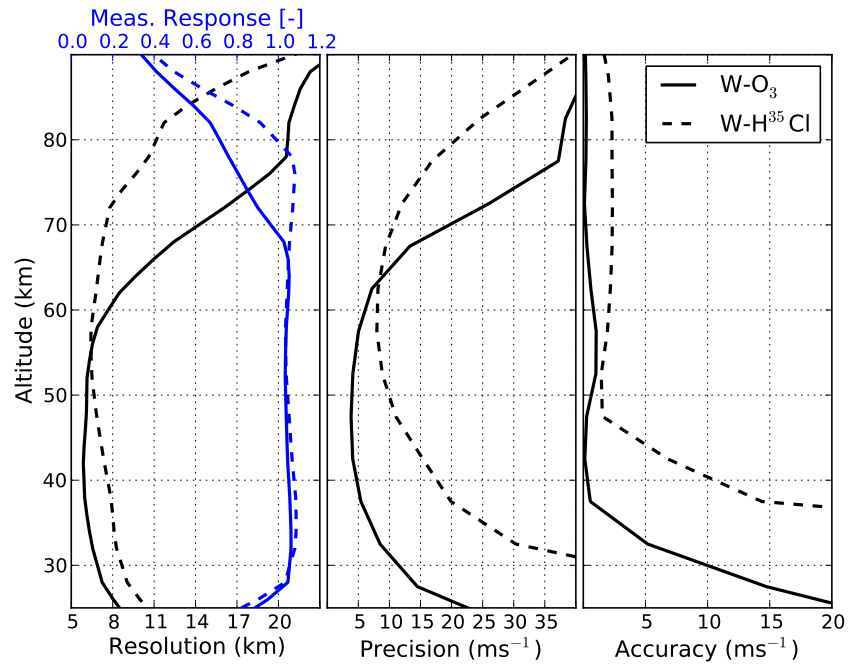


**Fig. 4.** Left panel: vertical resolution (dark line) and measurement response (blue line) for line-of-sight wind profiles retrieved from the O<sub>3</sub> spectral line (full lines) and from the H<sup>35</sup>Cl triplets in band B (dashed lines). Central panel: estimates of line-of-sight wind single retrieval precision derived from the O<sub>3</sub> spectral line (full line) and the H<sup>35</sup>Cl triplets (dashed line). Right panel: same as central panel but for the accuracy.

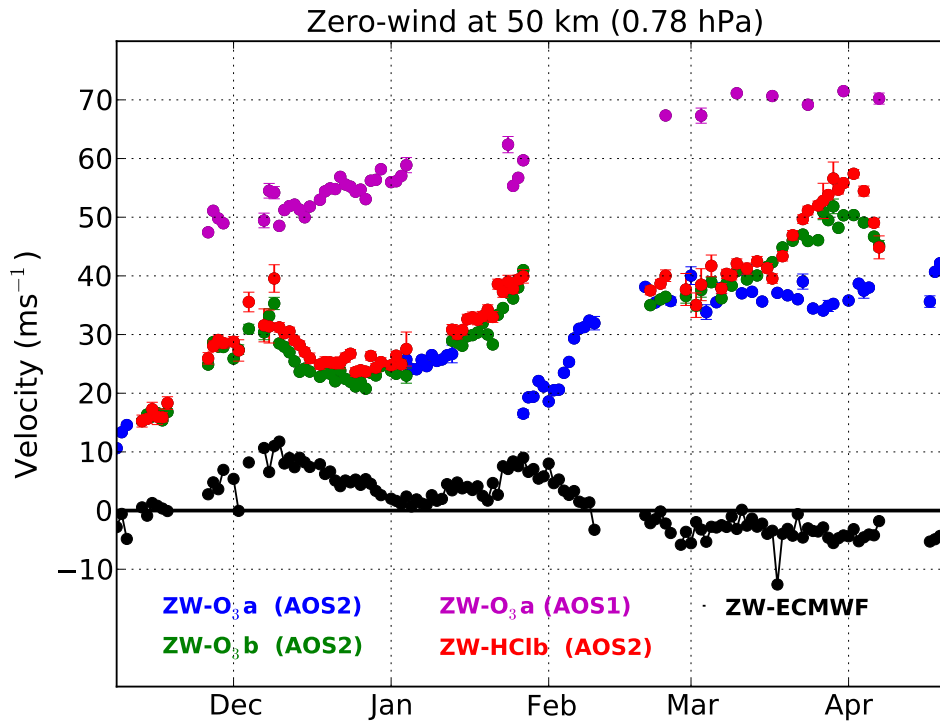


**Fig. 5.** Zero-wind for bias correction derived at 50 km from the O<sub>3</sub> line in band-A using spectrometer 1 (magenta dots) and spectrometer 2 (blue dots), the O<sub>3</sub> line in band-B and spectrometer 2 (green dots) and HCl line in band-B (red dots) along with the zero-wind computed with the paired ECMWF winds. The error bar corresponds to the retrieval errors of the averaged profiles (1-σ). The displayed zero-wind includes the subtraction of the ECMWF zero-winds.

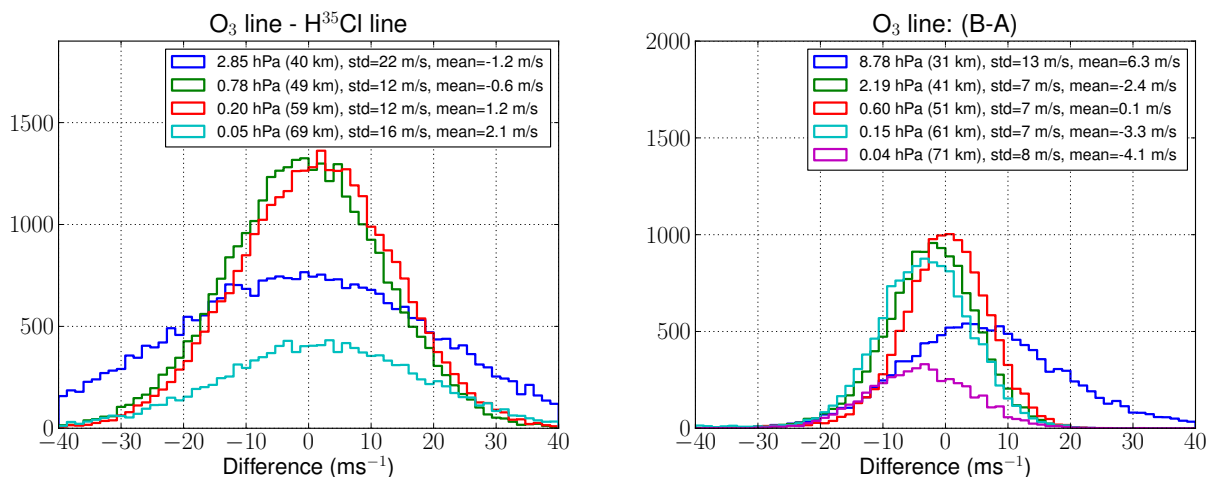


**Fig. 6.** Left panel: histogram of differences of the velocity retrieved from the O<sub>3</sub> and the HCl lines in band B. Right panel: same as for the left panel but for line-of-sight winds retrieved from the O<sub>3</sub> lines in bands A and B measured simultaneously. Data for latitudes between 20° N and 60° N have been used.

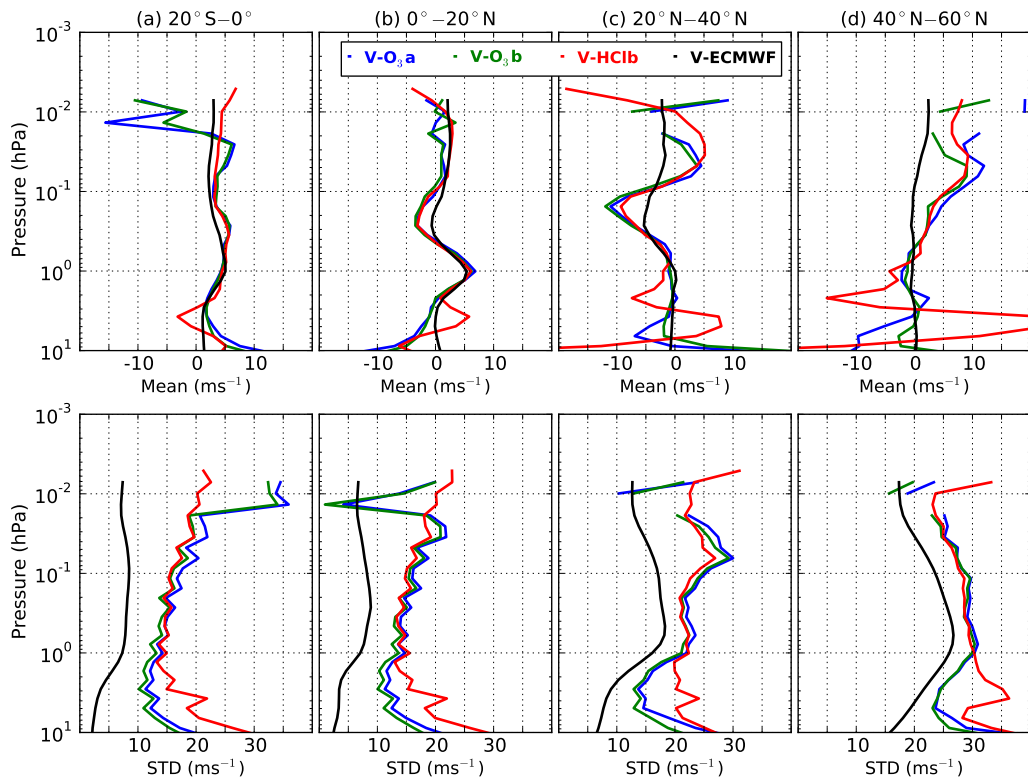


**Fig. 7.** Upper panels: zonally averaged near meridional wind profiles retrieved from simultaneous measurements of the spectral lines: O<sub>3</sub>-band A (blue line), O<sub>3</sub>-band B (red line) and HCl-band B (green line). Lower panels: same as the upper panels but showing the standard deviation of the retrieved profiles. The results for the paired ECMWF winds component along the line-of-sights are also shown (black line). Data with a line-of-sight orientation between  $\pm 10^\circ$  from the meridional direction are used.

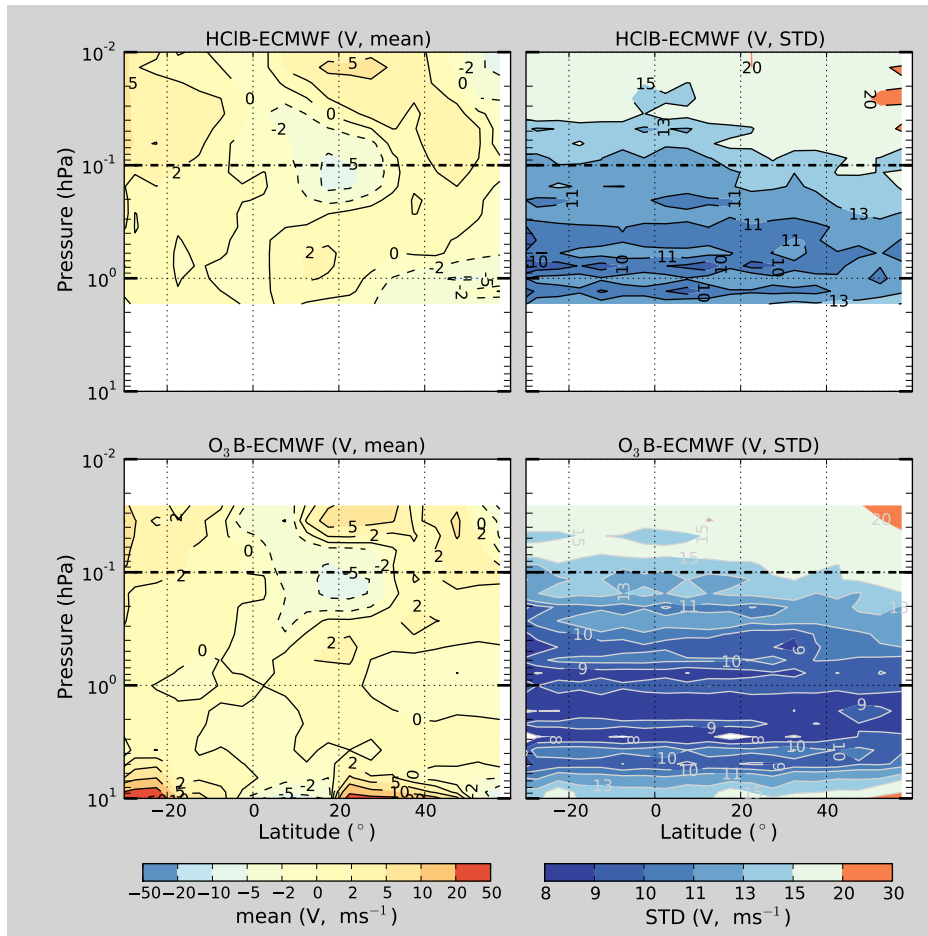


**Fig. 8.** Comparison of the near meridional winds retrieved from band-B with the operational ECMWF analysis. Data with a line-of-sight orientation between  $\pm 10^\circ$  from the meridional direction are used. ECMWF winds are projected along the line-of-sight direction. Upper panels: mean (left panel) and standard deviation (right panel) of the differences for profiles retrieved from the HCl lines. Lower panels: same as for the upper panels but for profiles retrieved from the O<sub>3</sub> line. Data between November 2009 to April 2010 have been selected.

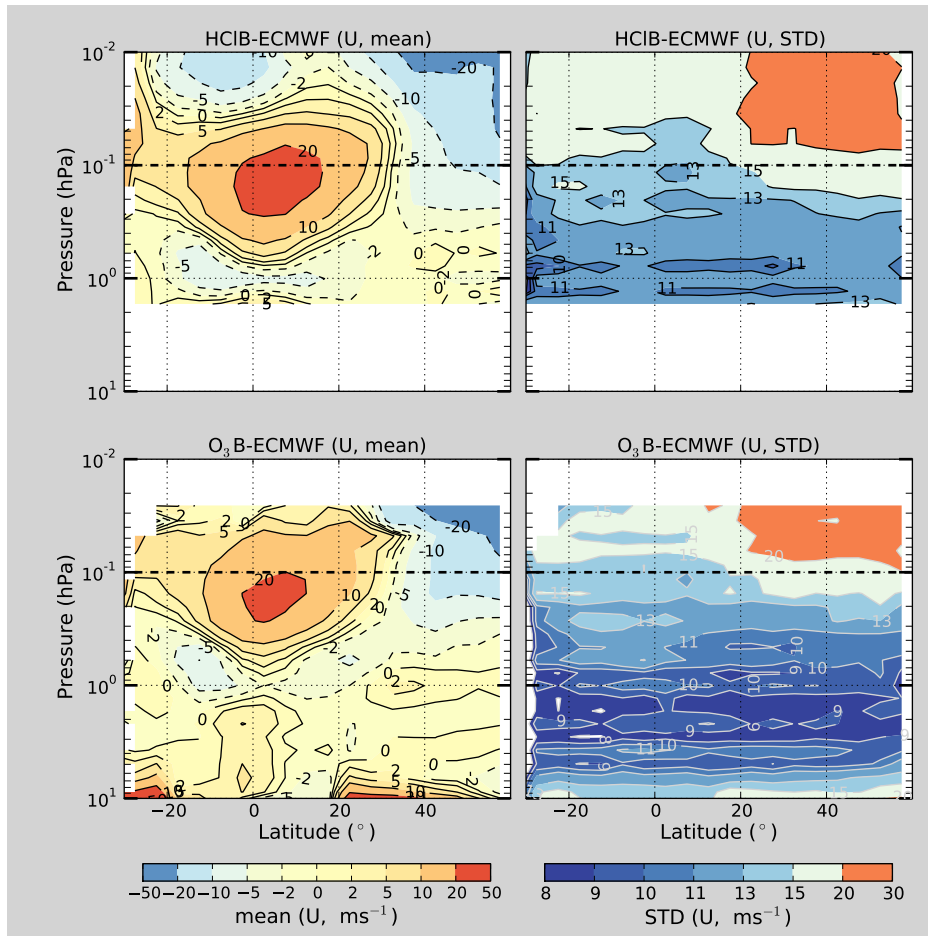


**Fig. 9.** Same as for Fig. 8 but for the near zonal component. Data with a line-of-sight orientation between  $\pm 10^\circ$  from the zonal direction are used.

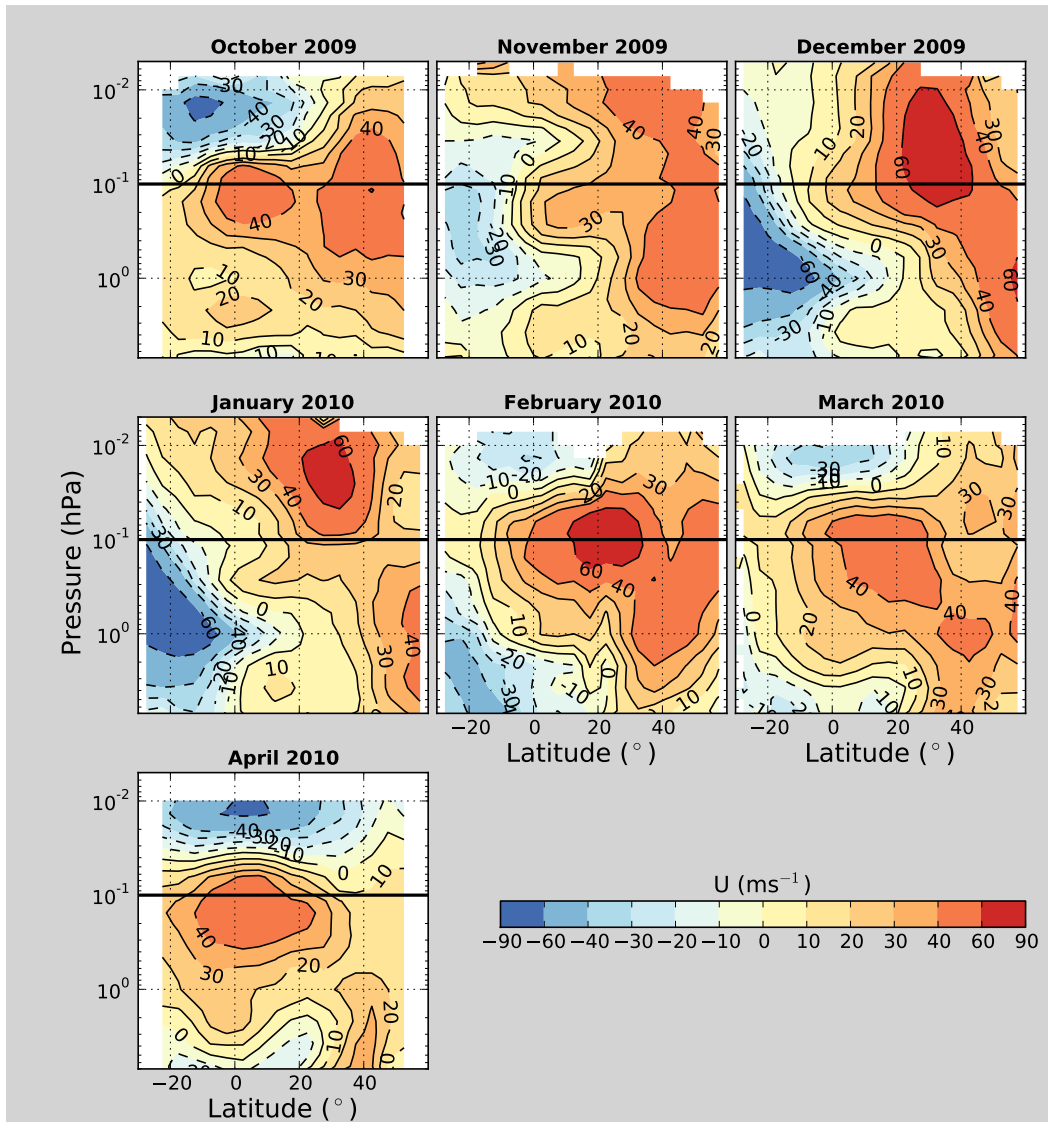


**Fig. 10.** Monthly and zonally averaged near zonal-wind derived from SMILES measurements in band B between October 2009 to April 2010. Wind information is taken from the  $O_3$  line retrieval for altitudes below 0.1 hPa (65 km) and from the HCl line retrieval above. Data with a line-of-sight orientation between  $\pm 10^\circ$  from the zonal direction are used.

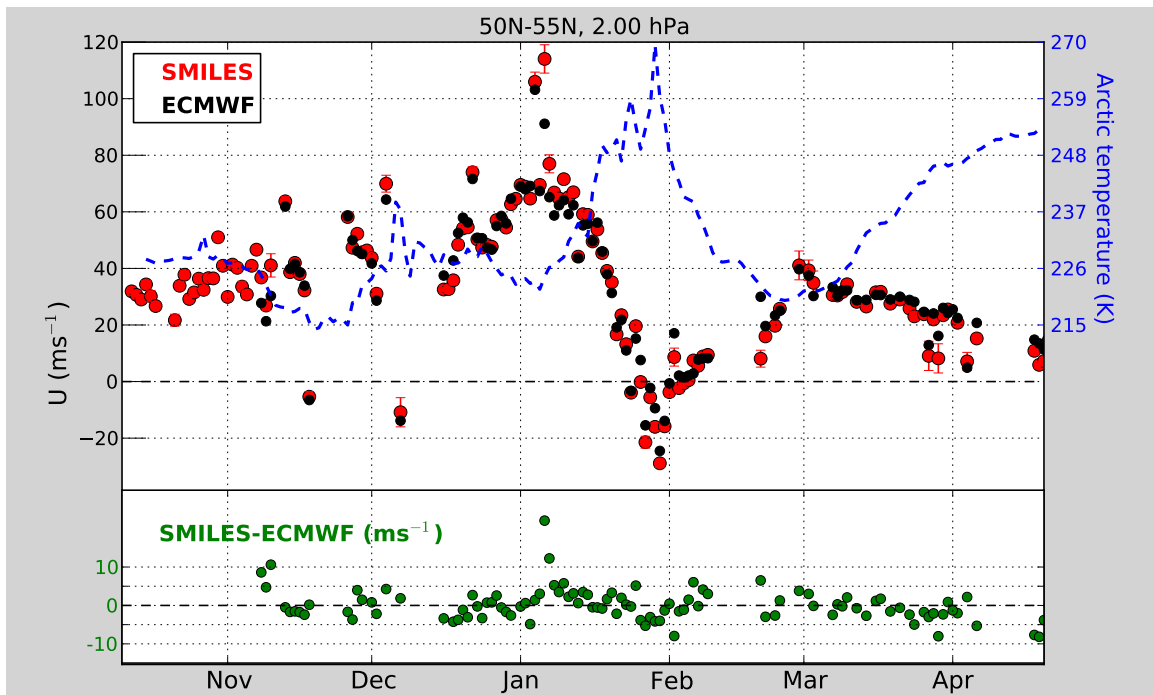


**Fig. 11.** Upper panel: daily-averaged SMILES zonal-wind in the northern high-latitudes at 2 hPa ( $\sim 41$  km) (red dots) and ECMWF analyses (black dots) between  $50^\circ\text{N}$ – $55^\circ\text{N}$ . SMILES winds are retrieved from the  $\text{O}_3$  line measured in band-B or in band-A if B is not measured. Data with a line-of-sight orientation between  $\pm 10^\circ$  from the zonal direction are used. ECMWF winds are projected on the line-of-sight. Temperature information (blue dashed line) is based on daily and zonally averaged MLS measurements between  $60^\circ\text{N}$ – $80^\circ\text{N}$ . Lower panels: difference SMILES-ECMWF.

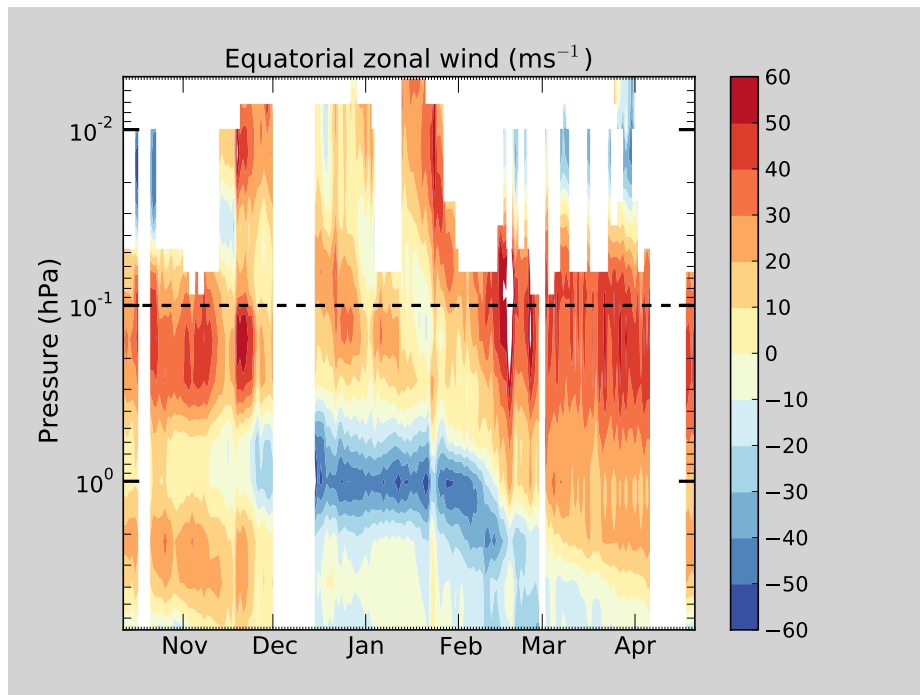


**Fig. 12.** The Semi-annual oscillation of the zonal winds over the equator ( $\pm 5^\circ$ ). Red regions correspond to eastward (westerly) winds. The winds from both the ozone and HCl lines are combined in the plot when band-B is measured: information is for  $O_3$  line below 0.1 hPa (65 km) and from HCl above. Information is from  $O_3$  when only band-A is measured. Data with a line-of-sight orientation between  $\pm 10^\circ$  from the zonal direction are used.

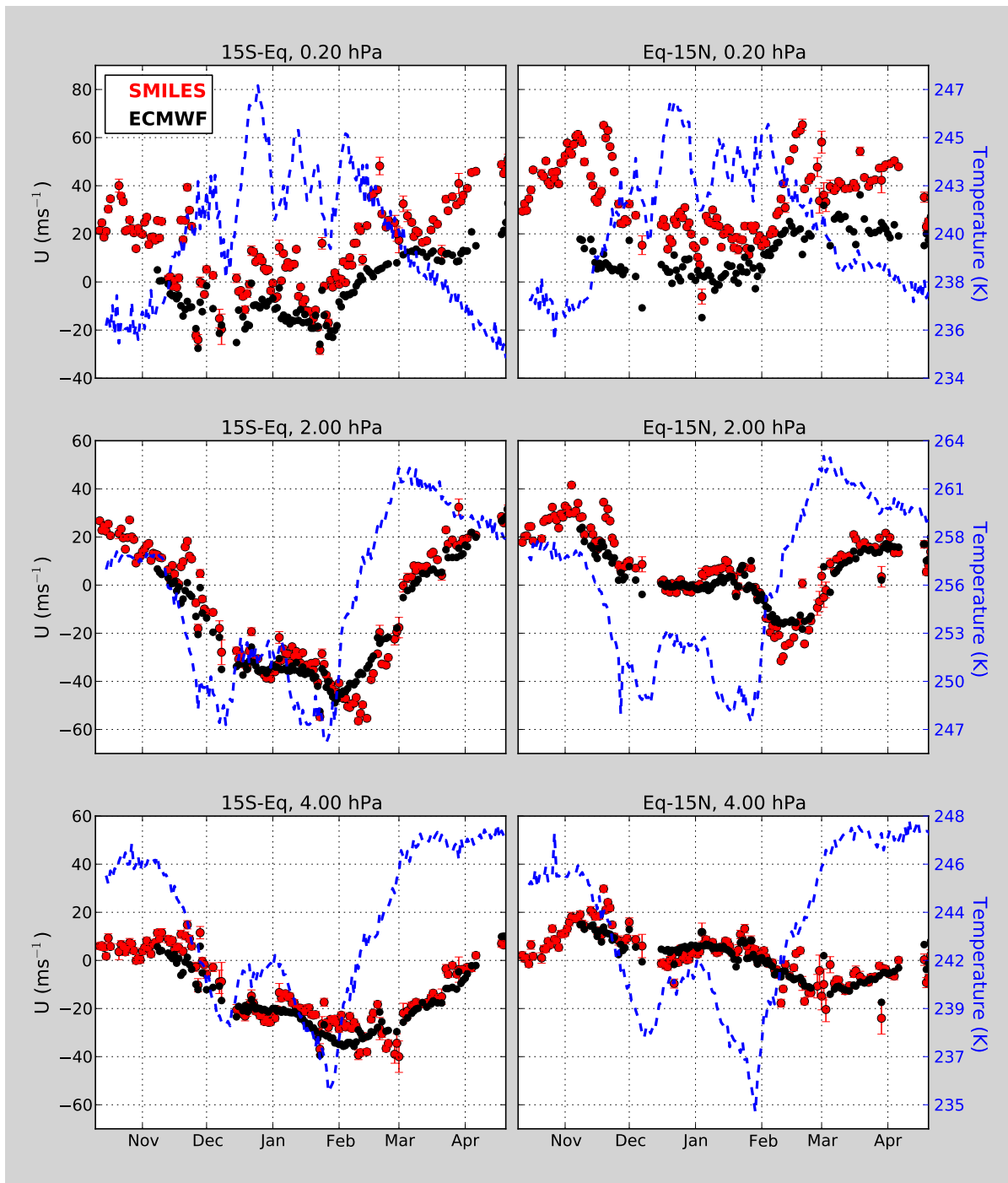


**Fig. 13.** Left panels: daily-averaged zonal-wind in the southern tropics ( $15^\circ \text{S}$ –Eq) at 4, 2 and 0.2 hPa ( $\sim 35$ , 41 and 60 km) derived from SMILES measurements (red dots) and ECMWF analyses (black dots). Data are retrieved from the  $\text{O}_3$  line in band-B or in band-A if B is not measured. Data with a line-of-sight orientation between  $\pm 10^\circ$  from the zonal direction are used. ECMWF winds are projected on the line-of-sight. The temperature profiles (blue dashed line) is a daily and zonal average of MLS measurements in the same latitudes range. Right panels: same as left panels but for the northern tropics.

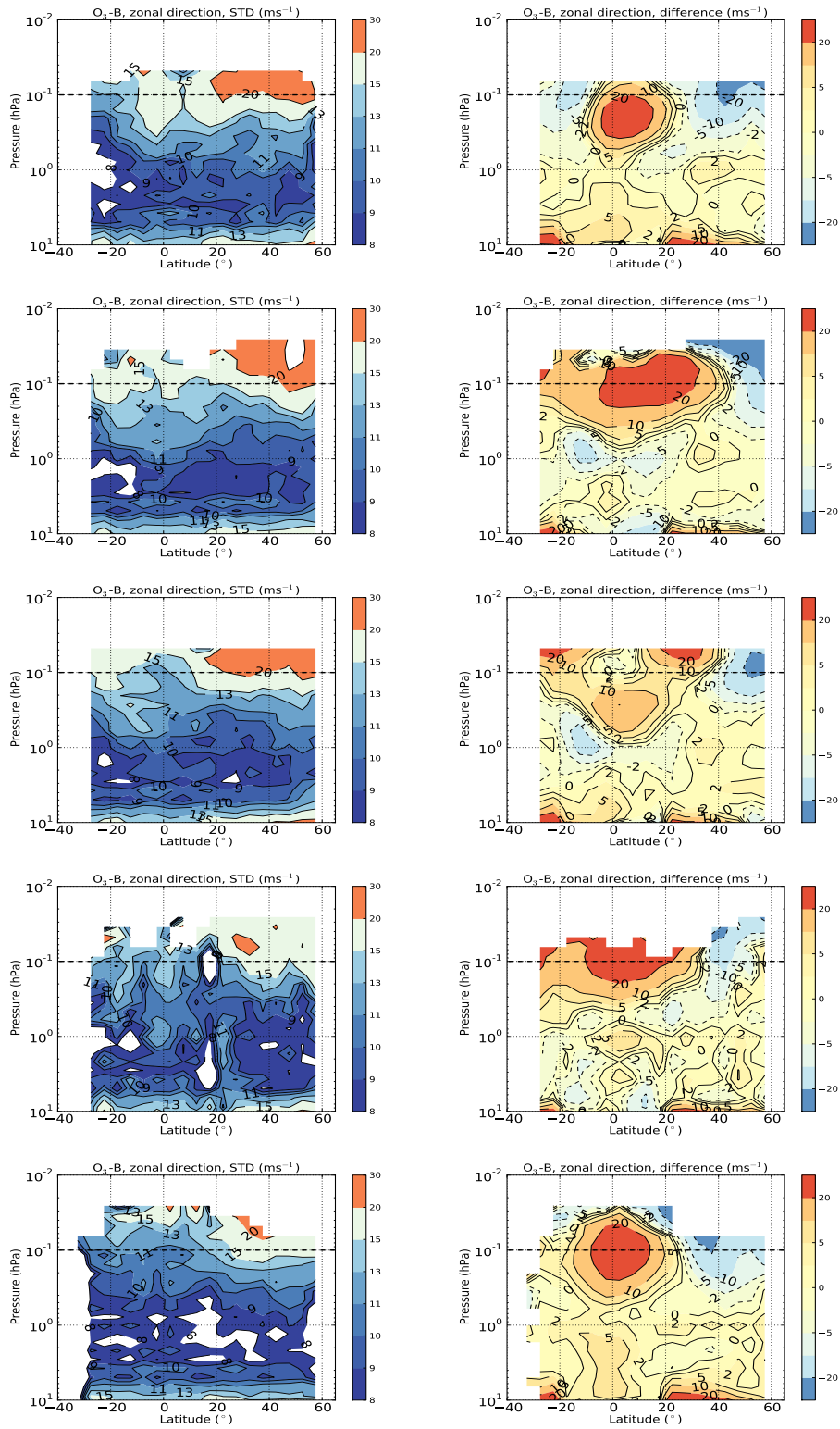


**Fig. 14.** Additional figure for discussion: SMILES-O3B zonal winds vs ECMWF from November to March (from top to bottom). The standard deviation and the mean of the differences are shown in the left and right columns, respectively.

## References

- Hays, P. B., Abreu, V. J., Dobbs, M. E., Gell, D. A., Grassl, H. J., and Skinner, W. R.: The High-Resolution Doppler Imager on the upper-atmosphere research satellite, *J. Geophys. Res.*, 98, 10713–10723, 1993.
- Killeen, T. L., Skinner, W. R., Johnson, R. M., Edmonson, C. J., Wu, Q., Niciejewski, R. J., Grassl, H. J., Gell, D. A., Hansen, P. E., Harvey, J. D., and Kafkalidis, J. F.: TIMED Doppler Interferometer (TIDI), optical spectroscopic techniques and instrumentation for atmospheric and space research III, *Proc. SPIE*, 3756, 289–301, doi:<http://dx.doi.org/10.1117/12.36638310.1117/12.366383>, 1999.
- McDade, I. C., Shepherd, G. G., Gault, W. A., Rochon, Y. J., McLandress, C., Scott, A., Rowlands, N., and Buttner, G.: The stratospheric wind interferometer for transport studies SWIFT), in: *Igarss 2001: Scanning the Present and Resolving the Future*, Vol. 3, Proceedings, 1344–1346, Sydney NSW, 9–13 July, doi:10.1109/IGARSS.2001.976839, 2001.
- Niciejewski, R., Wu, Q., Skinner, W., Gell, D., Cooper, M., Marshall, A., Killeen, T., Solomon, S., and Ortland, D.: TIMED Doppler interferometer on the Thermosphere Ionosphere Mesosphere Energetics and Dynamics satellite: data product overview, *J. Geophys. Res.-Space*, 111, A11S90, doi:10.1029/2005JA011513, 2006.
- Ortland, D. A., Skinner, W. R., Hays, P. B., Burrage, M. D., Lieberman, R. S., Marshall, A. R., and Gell, D. A.: Measurements of stratospheric winds by the High Resolution Doppler Imager, *J. Geophys. Res.*, 101, 10351–10363, 1996.
- Shepherd, G. G., Thuillier, G., Gault, W. A., Solheim, B. H., Hersom, C., Alunni, J. M., Brun, J. F., Brune, S., Charlot, P., Cogger, L. L., Desaulniers, D. L., Evans, W. F. J., Gattinger, R. L., Girod, F., Harvie, D., Hum, R. H., Kendall, D. J. W., Llewellyn, E. J., Lowe, R. P., Ohrt, J., Pasternak, F., Peillet, O., Powell, I., Rochon, Y., Ward, W. E., Wiens, R. H., and Wimperis, J.: WINDII, The wind imaging interferometer on the upper-atmosphere research satellite, *J. Geophys. Res.*, 98, 10725–10750, 1993.
- Stoffelen, A., Pailleux, J., Källén, E., Vaughan, J., Isaksen, L., Flamant, P., Wergen, W., Andersson, E., Schyberg, H., Culoma, A., Meynart, R., Endemann, M., and Ingmann, P.: The atmospheric dynamics mission for global wind field measurement, *B. Am. Meteorol. Soc.*, 86, 73–87, 2005.
- Swinbank, R. and Ortland, D. A.: Compilation of wind data for the Upper Atmosphere Research Satellite (UARS) Reference Atmosphere Project, *J. Geophys. Res.*, 108, 4615, 2003.
- Wu, D. L., Schwartz, M. J., Waters, J. W., Limpasuvan, V., Wu, Q. A., and Killeen, T. L.: Mesospheric doppler wind measurements from Aura Microwave Limb Sounder (MLS), *Adv. Space Res.*, 42, 1246–1252, 2008.